Group Theoretical Structure of Spectral Spaces

REINER LENZ AND THANH HAI BUI
Media Group, Campus Norrköping, Linköping University, Bredgatan, SE-60174 Norrköping, Sweden

JAVIER HERNÁNDEZ-ANDRÉS
Department of Optics, Sciences Faculty, University of Granada, 18071 Granada, Spain

Abstract. It is known that for every selection of illumination spectra there is a coordinate system such that all coordinate vectors of these illumination spectra are located in a cone. A natural set of transformations of this cone are the Lorentz transformations. In this paper we investigate if sequences of illumination spectra can be described by one-parameter subgroups of Lorentz-transformations. We present two methods to estimate the parameters of such a curve from a set of coordinate points. We also use an optimization technique to approximate a given set of points by a one-parameter curve with a minimum approximation error. In the experimental part of the paper we investigate series of blackbody radiators and sequences of measured daylight spectra and show that one-parameter curves provide good approximations for large sequences of illumination spectra.

1. Introduction

The description of properties of illumination spectra is of interest in many applications (see the introduction in [11] for an historical overview and applications). One important application in machine vision is the problem of color constancy. By assuming that the scene can be observed under a continuously changing illumination, the algorithm developed in [15] estimates the parameters describing the evolution of the changing illumination. The algorithm is based on the observation that there is a coordinate system in which the projected coordinates of the time-changing illumination spectra are located in a cone, and the assumption that these parameters can be described by a one-parameter subgroup operating on that cone.

In this paper we investigate the problem if relevant sets of illumination spectra are located on curves defined by one-parameter subgroups. This is an attempt to understand the structure of spaces of illuminations. The original motivation for these investigations came from the machine vision application mentioned above,

but the results should be of general interest and we will mention some applications at the end of the paper.

The paper is organized as follows: in Section 2 we briefly summarize the framework of conical coordinate systems of spectral spaces. These coordinate systems describe the chromatic properties of sequences of illumination spectra by sequences of points on the open unit disk. Some basic concepts of one-parameter subgroups operating on the unit disk are given in Section 3. Assuming that the input sequence of points forms a one-parameter subgroup, we introduce two group theoretical approaches (Sections 4.1 and 4.2 respectively) to recover the parameters characterizing the one-parameter subgroup. Relaxing this assumption, an optimization technique is then introduced to estimate a one-parameter curve describing the input data. In our experiments, described in Section 5, we investigate the properties of sets of blackbody spectra and measured daylight spectra. For the blackbody spectra we will show that there is a close relation between the one-parameter subgroup description and the mired parametrization (blackbody spectra are usually

characterized by the temperature of the corresponding blackbody, the unit of the reciprocal scale is called the mired and given by 10^6 K^{-1}). This is remarkable since it shows that there is a structural similarity to the mired representation (related to human color perception) but not to the temperature representation (derived from physics).

For the measured daylight spectra we will show that long stretches of the illumination spectra are located near one-parameter curves. We also show that there is a clear break when normal daylight changes to twilight. Both parts of these sequences can be described by (different) one-parameter curves. For the normal daylight spectra this is to be expected since daylight spectra don't change too much. The one-parameter group description gives however also a good description of the spectra in the twilight sequences when chromatic changes are very large. Although we did not derive an analytical relation between the spectral sequences and the one-parameter curves we found that the one-parameter curves provided good approximations. A longer discussion of the results obtained and a description of possible consequences and applications of these results is provided in the last section. Here we only mention that the group theoretical structure of the model makes it possible to apply all the tools from the Lie-theory of differential equations and abstract harmonic analysis. Examples are systematical and automatical constructions of all invariants under all changes described by groups, color constancy and tracking (see [15, 17, 21]). A summary of the basic facts about how to analyse spectra in the Hilbert space framework and a new derivation of the conical structure of the spectral spaces are given in the appendix.

2. The Conical Structure of Spectral Color Spaces

It is well known that illumination spectra can be described by linear combinations of only few basis vectors [9–11, 20, 24, 27, 32]. In many applications the eigenvectors of the input correlation matrix are taken as these basis vectors [4, 5, 14, 19, 22, 30, 32].

Denote in the following a spectral vector by $s(\lambda)$, basis vectors by $b_k(\lambda)$ and collect the coefficients in the vector σ, we thus have:

$$s(\lambda) \approx \sum_{k=0}^{K} \sigma_k b_k(\lambda). \qquad (1)$$

Under the condition that one of the basis vector is positive everywhere it can be shown that the vectors σ are located in a cone. A detailed description of the conditions under which this conical coordinate space is obtained are described in [15, 16] and the appendix. There we also discuss the relation between the spectra and their description by projection operators in detail. For all the spectral databases we investigated in the past we found that eigenvector-based systems (such as those used in this paper) are conical. In the following we will only use three basis vectors ($K = 2$). Higher order approximations of the illumination spectra which share the same conical properties are also possible but the group theoretical methods to investigate these coordinate vectors are more complicated. In the following we will thus concentrate on coordinate vectors located in the cone:

$$\mathcal{H} = \left\{ (\sigma_0, \sigma_1, \sigma_2) : \sigma_0^2 - \sigma_1^2 - \sigma_2^2 > 0 \right\}.$$

Conical or pyramid-shaped coordinate spaces are often used in color related applications although their conical structure is seldom emphasized. Examples are polar coordinates in the (a, b) plane together with non-negative L-coordinates in CIELAB and color systems of the HSV-type in image processing or computer graphics. Even the common RGB space can be seen as a pyramid if the diagonal in the RGB cube is used as the axis. Color theories based on the conical structure of color spaces were also developed in the framework of Lorentz transformations and we will discuss them briefly in the discussion part. All of these systems are however related to human color perception. In the context of this paper it is important to note that we are considering general collections of spectra and that each collection carries its own coordinate system. We are therefore not interested in the space of spectra as such but only in a given set of spectra. In this paper we select three such sets, the set of blackbody radiators and sets of daylight spectra measurements. Other collections of interest could be biologically relevant set of spectra [2, 3] or spectra relevant for an industrial inspection application.

Since the basis function $b_0(\lambda)$ is non-negative and since the coefficient σ_0 is the scalar product of the spectrum and $b_0(\lambda)$ it follows that σ_0 is related to the intensity of the spectrum. The projected coefficients $x = \sigma_1/\sigma_0$ and $y = \sigma_2/\sigma_0$ define a point z on the unit disk $\mathcal{U}$. We write these coordinates as points in

the complex plane:

$$\mathcal{U} = \{z : z = x + iy; \quad |z| < 1\}. \tag{2}$$

Since its location is independent of the intensity it can be considered as chromaticity coordinate of $s(\lambda)$.

3. One Parameter Subgroups and SU(1,1) Curves on the Unit Disk

In the following, we consider functions of the spectra (that are independent of the intensity) as functions of the complex variable z on the unit disk. The transformation from one spectrum to another can then be described as the transformation from a point z to another point w on this disk.

Special transformations of the disk are elements of $\mathbf{SU(1,1)}$, which is the group of all mappings that preserve the hyperbolic geometry (defined by the hyperbolic length and angle) of the Poincaré disk. For more information about hyperbolic geometry the interested reader may consult one of the many textbooks on the subject. For the basic facts needed in this paper the brief overviews in [26] and [8] are sufficient. The hyperbolic distance on the unit disk is given by:

$$d_h(z, w) = 2 * \text{arctanh} \frac{|z - w|}{|\bar{z} * w - 1|}; \quad z, w \in \mathcal{U}. \tag{3}$$

The transformations preserving this geometry are given by complex 2×2 matrices of the form:

$$\mathbf{SU(1,1)} = \left\{ \mathbf{M} = \begin{bmatrix} a & b \\ \bar{b} & \bar{a} \end{bmatrix}; \quad |a|^2 - |b|^2 = 1; \right.$$
$$\left. a, b \in \mathbb{C} \right\}. \tag{4}$$

An element $\mathbf{M} \in \mathbf{SU(1,1)}$ acts as the fractional transformation on points z on the unit disk:

$$w = \mathbf{M}\langle z \rangle = \frac{az + b}{\bar{b}z + \bar{a}}; \quad z, w \in \mathcal{U}. \tag{5}$$

These transformations preserve the hyperbolic length and we thus have:

$$d_h(z, w) = d_h(\mathbf{M}\langle z \rangle, \mathbf{M}\langle w \rangle); \quad z, w \in \mathcal{U} \tag{6}$$

We now introduce briefly some special subgroups of the group $\mathbf{SU(1,1)}$ and describe some of their most important properties. More information about Lie groups

and Lie algebras can be found in the relevant literature, such as [6, 21, 25, 31].

A one-parameter subgroup $\mathbf{M}(t)$ is a subgroup of $\mathbf{SU(1,1)}$, defined and differentiable for real values of t, having the properties:

$$\mathbf{M}(t_1 + t_2) = \mathbf{M}(t_1)\mathbf{M}(t_2) \; \forall t_1, t_2 \in \mathbb{R},$$
$$\mathbf{M}(0) = \mathbf{E} = \text{identity matrix}. \tag{7}$$

For a one-parameter subgroup $\mathbf{M}(t)$ we introduce its infinitesimal generator. It is represented by the matrix $\mathbf{X}$ defined as:

$$\mathbf{X} = \frac{d\mathbf{M}(t)}{dt}\bigg|_{t=0} = \lim_{t \to 0} \frac{\mathbf{M}(t) - \mathbf{E}}{t}. \tag{8}$$

Conversely, we can also construct a one-parameter subgroup $\mathbf{M}(t)$ from a given infinitesimal matrix $\mathbf{X}$ using the exponential map:

$$\mathbf{M}(t) = e^{t\mathbf{X}} = \mathbf{E} + t\mathbf{X} + \frac{t^2}{2!}\mathbf{X}^2 + \cdots + \frac{t^k}{k!}\mathbf{X}^k + \cdots \tag{9}$$

where $\mathbf{E}$ is the identity matrix. The infinitesimal matrices $\mathbf{X}$ form the Lie algebra su(1,1). Following the convention in Lie theory we will denote the group with capital letters and the corresponding algebra with lower case letters. The Lie algebra of the Lie group $\mathbf{SU(1,1)}$ is therefore denoted by su(1,1). It can be shown that this Lie algebra forms a three-dimensional vector space [25]. Each element in the Lie algebra has thus an expansion:

$$\mathbf{X} = \sum_{k=1}^{3} \xi_k \mathbf{J}_k. \tag{10}$$

where the $\mathbf{J}_k$ form the basis of the Lie algebra su(1,1) and are given by:

$$\mathbf{J}_1 = \frac{1}{2}\begin{bmatrix} 0 & 1 \\ 1 & 0 \end{bmatrix}; \quad \mathbf{J}_2 = \frac{1}{2}\begin{bmatrix} 0 & i \\ -i & 0 \end{bmatrix};$$
$$\mathbf{J}_3 = \frac{1}{2}\begin{bmatrix} i & 0 \\ 0 & -i \end{bmatrix}. \tag{11}$$

We use the vector of the three real numbers ξ_1, ξ_2 and ξ_3 to define the coordinate vector of $\mathbf{X}$.

Given a starting point $z(0)$ on the unit disk together with a one-parameter subgroup $\mathbf{M}(t)$ we define

a **SU(1,1)** curve as the following function of t:

$$z(t) = \mathbf{M}(t)\langle z(0)\rangle = \mathrm{e}^{t\mathbf{X}}\langle z(0)\rangle; \quad t \in \mathbb{R}; \quad z(t) \in \mathcal{U} \tag{12}$$

This curve is defined by the straight line $t\mathbf{X}$ in the three-dimensional Lie algebra. Although the restriction to one-parameter curves limits the class of curves on the chromaticity disk considerably we will show in the following that this class of curves is rich enough to provide interesting applications.

4.   Computing the Subgroup from the Spectra

Given a set of points $\{z_n = (x_n, y_n); n = 0, \ldots, N\}$ on the unit disk describing a series of illumination spectra, we describe algorithms to find a one-parameter subgroup (under the assumption that it exists) connecting these points. This is done by computing the Lie algebra $\mathbf{X}$ and the increment values Δt_n such that:

$$z_n = \mathbf{M}(\Delta t_n)\langle z_{n-1}\rangle = \mathrm{e}^{\Delta t_n \mathbf{X}}\langle z_{n-1}\rangle; \qquad n = 1, \ldots, N. \tag{13}$$

The Δt_n are the increments between two consecutive observations. We describe two methods to recover the one-parameter subgroup from a set that was generated by a one-parameter subgroup $\mathbf{M}(t)$. We first assume that the step length is fixed and given by Δt:

$$\exists \Delta t \in \mathbb{R}, \mathbf{X} \in \mathrm{su}(1,1) : \{z_n = \mathrm{e}^{\Delta t \mathbf{X}}\langle z_{n-1}\rangle;$$
$$n = 1, \ldots, N\}. \tag{14}$$

The general problem where no exact solution exists for the Eq. (13), will be solved with the help of an optimization technique at the end of this section. This is the case for real data which practically never lie exactly on a curve.

4.1.   Lie Algebra Method

Using the relation between the x, y coordinates, their first order derivatives and the three parameters of the **SU(1,1)** curve, we can recover the three coordinates ξ_1, ξ_2 and ξ_3 describing the one-parameter subgroup $\mathbf{M}(t) = \exp(t\mathbf{X})$ by solving the following linear equations:

$$\begin{bmatrix} \frac{1-x_k^2+y_k^2}{2} & -x_k y_k & -y_k \\ -x_k y_k & \frac{1+x_k^2-y_k^2}{2} & x_k \end{bmatrix} \begin{bmatrix} \xi_1 \\ \xi_2 \\ \xi_3 \end{bmatrix}$$
$$= \begin{bmatrix} \Delta x_k \\ \Delta y_k \end{bmatrix}. \tag{15}$$

Where $z_k = x_k + iy_k$, and Δx_k, Δy_k are the partial derivatives of the curve at z_k in x and y coordinates. The values of the partial derivatives can be computed by convolving a first order derivative kernel with the data set. The detailed description of the method can be found in [15]. From two observations z_{k-1}, z_k we obtain thus two equations. Given that ξ_1, ξ_2 and ξ_3 are varying slowly along the curve, we can obtain more equations from neighboring points and use all of them to estimate values of ξ_1, ξ_2 and ξ_3.

4.2.   Cartan Decomposition Method

In the following we denote the subgroup of rotations by K and the subgroup of hyperbolic transformations by $A^+ \in \mathbf{SU(1,1)}$:

$$K = \left\{ \mathbf{K}(\theta) = \begin{bmatrix} \mathrm{e}^{i\theta/2} & 0 \\ 0 & \mathrm{e}^{-i\theta/2} \end{bmatrix}; \quad 0 < \theta < 4\pi \right\}, \tag{16}$$

and

$$A^+ = \left\{ \mathbf{A}(\tau) = \begin{bmatrix} \cosh(\tau/2) & \sinh(\tau/2) \\ \sinh(\tau/2) & \cosh(\tau/2) \end{bmatrix}; \quad \tau \in \mathbb{R}^+ \right\}. \tag{17}$$

Then $G = KA^+K$ is the Cartan decomposition of **SU(1,1)**(for more information about this, and related, decompositions see [7, 28]). By this we mean that each $\mathbf{M} \in \mathbf{SU(1,1)}$ can be written as $\mathbf{M} = \mathbf{K}(\phi)\mathbf{A}(\tau)\mathbf{K}(\psi)$ for $\mathbf{K}(\phi), \mathbf{K}(\psi) \in K$; $\mathbf{A}(\tau) \in A^+$. If $\mathbf{M} \in \mathbf{SU(1,1)}$, and $\mathbf{M} \notin K$, this decomposition is unique. The relations between ϕ, τ, ψ and a, b are given by:

$$\tau = 2\mathrm{arctanh}\left|\frac{b}{a}\right|; \quad \phi = \arg\left(\frac{b}{\bar{a}}\right); \quad \psi = \arg(a\bar{b}), \tag{18}$$

or alternatively

$$a = e^{i(\phi+\psi)/2} \cosh \frac{\tau}{2}; \quad b = e^{i(\phi-\psi)/2} \sinh \frac{\tau}{2}. \quad (19)$$

Notice that $\mathbf{M}\langle 0 \rangle = (a \cdot 0 + b)/(\bar{b} \cdot 0 + \bar{a}) = b/\bar{a}$. We also have:

$$\tau = 2\mathrm{arctanh}\,|\mathbf{M}\langle 0 \rangle|\,; \quad \phi = \arg(\mathbf{M}\langle 0 \rangle)\,. \quad (20)$$

Consider first the simplest case with the special input set of three points $\{0, u, w\}$, where $0 < u < 1$. We construct an $\hat{\mathbf{M}} \in \mathbf{SU(1,1)}$ with:

$$u = \hat{\mathbf{M}}\langle 0 \rangle; \quad w = \hat{\mathbf{M}}\langle u \rangle; \quad 0 < u < 1; \ w \in \mathcal{U},$$
$$\hat{\mathbf{M}} = \mathbf{K}(\phi_M)\mathbf{A}(\tau_M)\mathbf{K}(\psi_M). \quad (21)$$

From Eq. (20), the first Eq. in (21) and using $u \in \mathbb{R}^+$ we get the values of the two parameters ϕ_M and τ_M:

$$u = \hat{\mathbf{M}}\langle 0 \rangle = \mathbf{K}(\phi_M)\mathbf{A}(\tau_M)\mathbf{K}(\psi_M)\langle 0 \rangle,$$

therefore

$$\phi_M = \arg(u) = 0; \ \tau_M = 2\mathrm{arctanh}(u). \quad (22)$$

Inserting this solution into the second Eq. in (21), we find for the third parameter ψ_M, from which we can compute $\mathbf{M}$:

$$w = \hat{\mathbf{M}}\langle u \rangle = \mathbf{K}(0)\mathbf{A}(\tau_M)\mathbf{K}(\psi_M)\langle u \rangle$$
$$= \mathbf{A}(\tau_M)\mathbf{K}(\psi_M)\langle u \rangle$$
$$= \mathbf{A}(\tau_M)\mathbf{K}(\psi_M)\mathbf{A}(\tau_M)\mathbf{K}(\psi_M)\langle 0 \rangle$$
$$= \mathbf{A}(\tau_M)\mathbf{K}(\psi_M)\mathbf{A}(\tau_M)\langle 0 \rangle,$$

therefore

$$\mathbf{K}(\psi_M)\mathbf{A}(\tau_M)\langle 0 \rangle = \mathbf{A}(\tau_M)^{-1}\langle w \rangle, \quad \text{and}$$
$$\psi_M = \arg(\mathbf{A}(\tau_M)^{-1}\langle w \rangle). \quad (23)$$

In the general case with arbitrary three points z_0, z_1 and z_2 on the unit disk related by a one-parameter subgroup, we want to find an $\mathbf{M} \in \mathbf{SU(1,1)}$: $z_1 = \mathbf{M}\langle z_0 \rangle$; $z_2 = \mathbf{M}\langle z_1 \rangle$.

First we show that there is an $\mathbf{N}_0 \in \mathbf{SU(1,1)}$ and $0 < u < 1; \ w \in \mathcal{U}$ such that:

$$z_0 = \mathbf{N}_0\langle 0 \rangle; \quad z_1 = \mathbf{N}_0\langle u \rangle; \quad z_2 = \mathbf{N}_0\langle w \rangle. \quad (24)$$

The matrix $\mathbf{M}$ connecting z_0, z_1 and z_2 can then be obtained by:

$$\mathbf{M} = \mathbf{N}_0\hat{\mathbf{M}}\mathbf{N}_0^{-1}. \quad (25)$$

where, by the same notation, $\hat{\mathbf{M}}$ is the solution of Eqs. (22), (23). $\mathbf{N}_0$ can be obtained by computing its Cartan parameters as follows:

$$z_0 = \mathbf{K}(\phi_N)\mathbf{A}(\tau_N)\mathbf{K}(\psi_N)\langle 0 \rangle$$
$$= \mathbf{K}(\phi_N)\mathbf{A}(\tau_N)\langle 0 \rangle,$$
$$\text{therefore } \phi_N = \arg(z_0); \ \tau_N = 2\mathrm{arctanh}|z_0|,$$
$$\text{then } z_1 = \mathbf{K}(\phi_N)\mathbf{A}(\tau_N)\mathbf{K}(\psi_N)\langle u \rangle \text{ gives}$$
$$\mathbf{A}(\tau_N)^{-1}\mathbf{K}(\phi_N)^{-1}\langle z_1 \rangle = \mathbf{K}(\psi_N)\langle u \rangle$$
$$= \mathbf{K}(\psi_N)\mathbf{A}(\tau_M)\mathbf{K}(\phi_M)\langle 0 \rangle,$$
$$\text{so } \psi_N = \arg((\mathbf{K}(\phi_N)\mathbf{A}(\tau_N))^{-1}\langle z_1 \rangle). \quad (26)$$

For given t and $\mathbf{M} = \exp(t\mathbf{X})$, we obtain the coordinates ξ_1, ξ_2, ξ_3 using Eqs. (10) and (11) as follows:

$$\begin{bmatrix} \xi_1 i & \xi_2 + \xi_3 i \\ \xi_2 - \xi_3 i & -\xi_1 i \end{bmatrix} = \mathbf{X} = \frac{\log(\mathbf{M})}{t},$$

therefore

$$\xi_1 = \frac{a_x}{i}; \quad \xi_2 = \frac{b_x + \overline{b_x}}{2}; \quad \xi_3 = \frac{b_x - \overline{b_x}}{2i},$$

where

$$\begin{bmatrix} a_x & b_x \\ \overline{b_x} & \overline{a_x} \end{bmatrix} = \mathbf{X}. \quad (27)$$

4.3.   Optimization as Linear Regression on the Unit Disk

For real data, the projected points on the unit disk are practically never exactly located on an $\mathbf{SU(1,1)}$ curve. We thus have to use an approximation. Given a set of points $\{z_n = (x_n, y_n); n = 1, \ldots, N\}$ on the unit disk describing a series of illumination spectra we formulate the problem of fitting the data to a $\mathbf{SU(1,1)}$ curve as an optimization problem as follows:

Find a series of parameters $\Delta t_n (n = 1, \ldots, N)$, a matrix $\mathbf{X}$ in su(1,1) and a point z_0 such that:

$$\sum_{n=1}^{N} d_h\big(z_n, \mathrm{e}^{(\tau_n \mathbf{X})} \langle z_0 \rangle\big) \quad \text{is minimal} \qquad (28)$$

where $\tau_n = \sum_{l=1}^{n} \Delta t_l$.

Here $\exp(\tau_n \mathbf{X}) \langle z_0 \rangle$ denotes the fractional linear transform of the matrix $\exp(\tau_n \mathbf{X})$ applied to the point z_0, and $d_h(z, w)$ (Eq. (3)) is the hyperbolic distance (which is invariant under the action of $\mathbf{SU(1,1)}$) between two points z and w on the unit disk.

In our implementation, we use the two methods described above to find the initial values for $\mathbf{X}$. These initial values are taken as the mean of all solutions given by applying the algorithms for all three consecutive points in the input set. Optimization is done using the Matlab Optimization Toolbox. The result of the optimization defines the projection of the input data set to the best fitting $\mathbf{SU(1,1)}$ curve.

5.   Experiments

In our experiments we investigate the properties of Planck black-body radiation spectra and measured sequences of daylight spectra.

5.1.   *Properties of the Sets of Black-Body Radiation*

In the first series of experiments we investigate the blackbody radiation spectra given by Planck's Eq. (29).

$$E(\lambda, T) = \frac{2\pi h c^2}{\lambda^5 (\mathrm{e}^{(hc/\lambda kT)} - 1)}. \qquad (29)$$

In which:

- h: Planck's constant (6.626×10^{-34} Js).
- c: Speed of Light (3×10^{8} m/s).
- λ: Wavelength (m).
- k: Boltzmann Constant (1.38×10^{-23} J/K).
- T: Temperature (K).

The goal of this experiment was to test whether the proposed framework is applicable in a simple but nontrivial case. Here we know the spectra in the database completely and could use known approximations, such as the Wien approximation (see [32]). The experiment is however interesting for at least two reasons:

- If the subgroup description gives a reasonable approximation then this is an indication that the methodology is useful since the derivation of the subgroup approximation is completely data-driven: The basis is computed by principal component analysis and the subgroup parameters are estimated from the expansion coefficients. From the definition of the blackbody radiation it is not immediately clear that there is such a group theoretical description and we will also show that the group parameter is similar to the inverse temperature and not to the temperature.
- The parametrization of the Planck spectra with one parameter is useful in practical applications like visualization. Here the decomposition of the spectral distribution into a linear combination and the simple rule how to change the relation between the weight coefficients can be used to pre-compute those parts of the data that depend on the basis functions and combine them with the different weight combinations to produce the final result.

In the following we use a reciprocal color temperature scale, i.e. $E(\lambda, \tau) = E(\lambda, 1/T)$. This parametrization is more linear with respect to human perception (see [29] and [32] pages 224–225), in the sense that a given small parameter change in this scale leads to similar perceptual change independent of the location in the parameter space. The unit of this reciprocal temperature scale is the mired (given by 10^6 K^{-1}) also known as reciprocal megakelvin.

In our experiments, we proceed as follows:

- First we generate a series of N Planck blackbody radiation spectra evenly distributed along the reciprocal color-temperature scale corresponding to the Kelvin range of $[T_{\mathrm{low}} .. T_{\mathrm{high}}]$, we denote this series as $S_{\mathrm{mired}}(N, T_{\mathrm{low}}, T_{\mathrm{high}})$. The correlation matrix of the sequence $S_{\mathrm{mired}}(5000, 3000, 200000)$ is used to compute the principal eigenvectors defining the basis.
- Then we generate new series of spectra with different parameters. Using the basis computed from the previous step, we compute the projected coefficients of the whole series resulting in a sequence of points on the unit disk $\{z(k) : z(k) \in \mathcal{U}, k = 1 \ldots N\}$.
- For each point $z(k)$ together with its neighbors, we apply the methods described above to find the three parameters $\xi_1(k), \xi_2(k), \xi_3(k)$ describing the estimated $\mathbf{SU(1,1)}$ curve.
- From an arbitrary point $z(k)$ from the input set and the one-parameter subgroup described by the computed

parameters $\xi_1(k), \xi_2(k), \xi_3(k)$ we use an optimization procedure to generate one simulated **SU(1,1)** curve describing the whole set.

- There are two different types of errors in the estimation of an illumination spectrum in the input sequences: The errors caused by approximating the illumination spectra with a few basis vectors, and the errors caused by estimating the coordinates of the spectrum by an **SU(1,1)** curve. In the experiments, we calculate for each spectrum in the input sequence:

1. **Hyperbolic estimation error:** $\mathcal{H}_e(k) = h_d(w(k), z(k))$.

2. L^2 **approximation error:** $\mathcal{L}_a^2(k) = \| \sum_{j=0}^{2} \sigma_j^z(k) b_j - s(k) \|$.

3. L^2 **estimation error** $\mathcal{L}_e^2(k) = \| \sum_{j=0}^{2} \sigma_j^w(k) b_j - s(k) \|$.

where b_j is a basis vector, $z(k)$ and $w(k)$ are the coordinates of the spectrum k and its **SU(1,1)** estimation, $s(k)$ is the kth spectrum and $\sigma_j^z(k), \sigma_j^w(k)$ are the jth coefficients of $z(k)$ and $w(k)$ respectively.

- Figures 1 and 2 show the results when we apply the estimation to the different series of Planck spectra ($S_{\text{mired}}(300, 4000, 15000)$ in Fig. 1 and $S_{\text{mired}}(500, 5000, 20000)$ in Fig. 2) and different
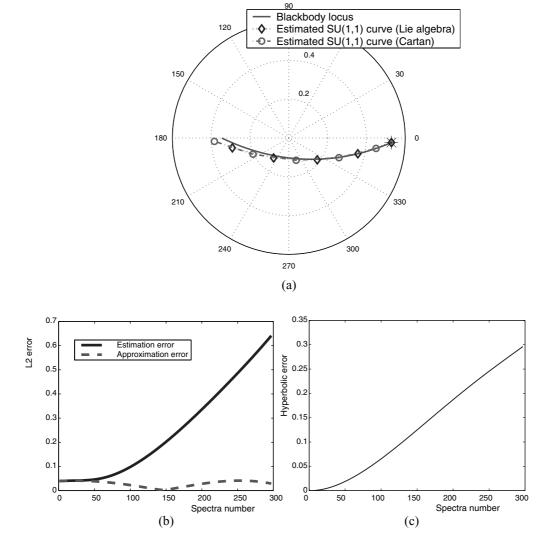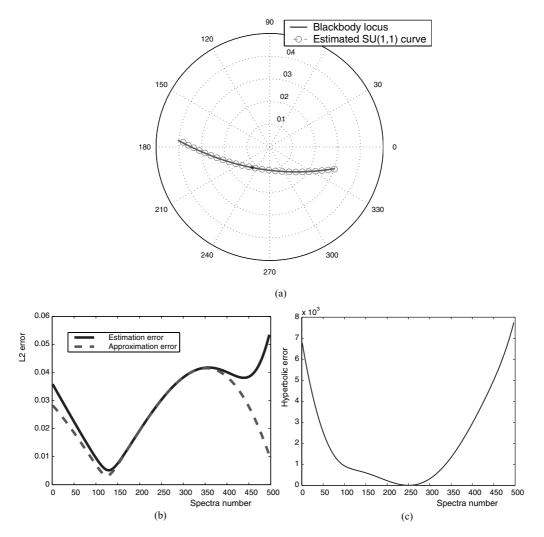

Figure 1. Blackbody spectra sequence estimation: 300 samples in the interval 4000..15000 K, equally spaced in mired scale; starting point 1st spectrum in the sequence (4000 K). (a) Blackbody locus and the estimated **SU(1,1)** curve on the unit disk, (b) Relative approximation and estimation errors, (c) Hyperbolic estimation error.

Figure 2.   Blackbody spectra sequence estimation, 500 samples in the range 5000..20000 K, equally spaced in mired scale, starting point: 250th spectrum in the sequence (7990 K). (a) Blackbody locus and the estimated **SU(1,1)** curve on the unit disk, (b) Relative approximation and estimation errors, (c) Hyperbolic estimation error.

starting points. The L^2 estimation/approximation and the hyperbolic estimation error distributions are shown in part (b) and part (c) of those figures respectively. In Fig. 1(a) we show as solid line the chromaticity location of the original Planck spectra. The results of the estimations based on the Cartan decomposition are shown as dashed line (marked with circles every 60th spectrum), the Lie-algebra based results are plotted as dotted line (marked with diamonds every 60th spectrum). This shows that there is practically no difference between the results obtained by these two methods. We therefore present only results computed with the Cartan decomposition in Fig. 2 (marked with circles every

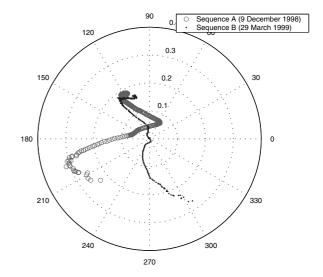20th spectrum). Also the error distributions shown in parts (b) and (c) are obtained with the Cartan method.

In Fig. 1 we start tracking the illumination changes at the first spectrum in the sequence and the estimation error accumulates over the sequence, whereas in Fig. 2 we start tracking in the middle of the sequence in both directions. The estimation error is much lower compared to the previous result (note the different scalings in the two figures).

From our experiments with different numbers of Planck spectra, temperature ranges, and starting points $z(s)$ we draw the following conclusions:

- The reciprocal scaled series of Planck spectra can be well described by a one parameter subgroup with fixed Δt.
- The Cartan decomposition and the Lie algebra methods give essentially the same results when we choose the sampling rate high enough. The Lie algebra method provides better approximation in the case of a low sampling rate (e.g. 30 samples taken in the range between [4000 K..15000 K]).
- The approximation error caused by the reconstruction of the spectra from the KLT coordinates can be limited if the temperature range used to compute the basis is larger than the range of the series being described. The range [3000 K..200000 K] is chosen for the basis since it covers the majority of illumination sources of interest for this paper (see [32], page 28).
- Theoretically there is no **SU(1,1)** curve perfectly describing the Planck spectra series, but the L^2 approximation/estimation errors are relatively small (with an average error of less than 1% as can be seen in Figs. 1(b), 2(b)) when we choose the starting point in the middle of the series (Fig. 2).

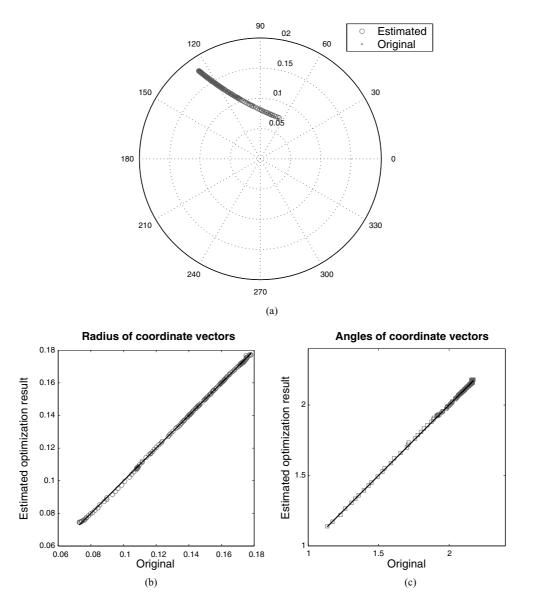### 5.2. *Properties of Measured Time-Sequence Daylight Spectra*

We also investigated sequences of time-changing daylight illumination spectra measured in Granada, Spain (37 ° 11′ N, 3°37′ W, altitude: 680 m, see [10, 11, 13]). The correlation matrix of the measured daylight spectra is used to compute three principal eigenvectors for this basis. The projected coordinates of such a sequence on the unit disk are also computed, defining the vectors $\{z_k : k = 1..N\}$. Figure 3 shows the location of daylight illumination spectra sequences measured on two different clear-sky days. Sequence A has 433 illumination spectra, measured on 9-December-1998, where the first 185 spectra are measured every minute (solar elevations from 30.0° -the maximum for that day- to 15.5°) and the remaining spectra were collected every 30 seconds (solar elevations from 15.0° to −5.5° -approximately the end of civil twilight-). The first 271 of 368 spectra in sequence B, measured on 29-March-1999, were collected every minute during daylight (solar elevations from 56.0° -the maximum for that day- to 5.4°) and the remaining every 30 seconds during twilight (solar elevations from 4.6° to −4.7°). A detailed investigation of these, and other, measurements can be found in [11] and [13].

Figure 3. Projected coordinates of the daylight spectra measured in Granada on the unit disk.

We investigated the properties of these measured illumination spectra by applying the optimization technique described above to different subsequences taken from the input set. The sum of the hyperbolic distances between the original and estimated points (its projection on the estimated curve) is used as a cost function for the optimization.

At certain points in time, the Granada curves change direction, which means that another **SU(1,1)** curve describing this new portion has to be found. We call these points break points. The positions of the break points are located manually in the experiments described in this article. The first section of the measurement series near the origin represents the daylight spectra whereas the long tails of the sequences originate in the twilight spectra. The break points corresponds roughly to those points in time when ordinary daylight goes over to the very differently colored twilight spectra. See [13] for details on these and other twilight measurements. Figures 4 and 5 show the results of the optimization with different subsequences taken from the Granada sequences. The figures show the coordinates of the input illumination spectra subsequence and the estimated **SU(1,1)** curve. The radial and angular values of the input illumination coordinate points and its **SU(1,1)** estimation are illustrated in the parts (b) and (c) of those figures. The horizontal axis shows the value of the variable of the original input spectra and the vertical axis the estimation. For perfect estimation, the points should be located on
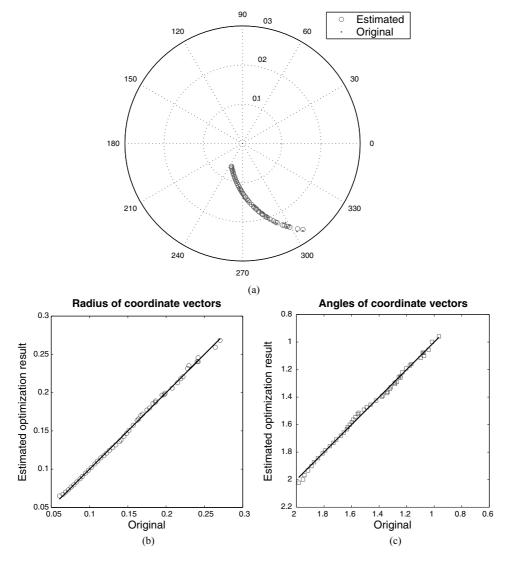
Figure 4. Estimated and original coordinates of Granada sequence A, subsequence: spectrum 180 to spectrum 330. (a) Daytime illumination sequence and estimated **SU(1,1)** curve, (b) Radius of coordinate vectors of the daytime illumination sequence versus estimation, (c) Angles of coordinate vectors of daytime illumination sequence versus estimation.

the 45° line, which is presented by a solid line in the figures.

We found that:

- Among the first spectra in the input sequences A and B (first 180 spectra in sequence A and 110 spectra in sequence B) there is almost no coordinate change. Those spectra belong to daylight measurements for high solar elevations.

- Long subsequences of spectra with time changing coordinates in both sequences A and B can be described by **SU(1,1)** curves. Two examples are illustrated in Fig. 4, (sequence A, 151 spectra measured with solar elevations between 16.2° and 3.6°) and Fig. 5 (sequence B 49 spectra with solar elevations between 0.1° and −4.7°). These subsequences represent the color changes during sunset. For the sunset part of sequence A (91 spectra with solar elevations

Figure 5. Estimated and original coordinates of Granada set B, subsequence: spectrum 320 to spectrum 368. (a) Daytime illumination sequence and estimated **SU(1,1)** curve, (b) Radius of coordinate vectors of daytime illumination sequence versus estimation, (c) Angles of coordinate vectors of daytime illumination sequence versus estimation.
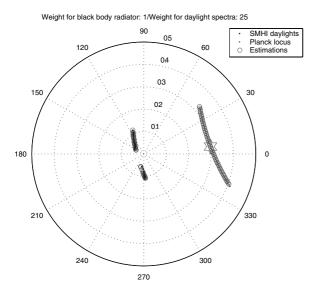
between $3.6°$ and $-4.4°$) and other subsequences the results are similar and are therefore not shown here.

5.3. Properties of Combined Databases of Blackbody and Daylight Spectra

Another database we used in our experiments is a database with 21871 daylight spectra (measured by SMHI, the Swedish Meteorological and Hydrological Institute in Norrköping, Sweden, ($58°35'$ N, $16°09'$ E, altitude: 34 m). The data was gathered from June 16th,
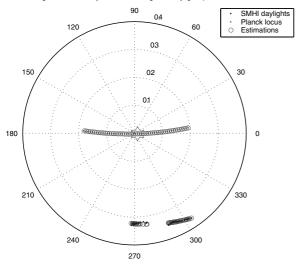
1992 to July 7th, 1993 during daytime (varies between 5:10 and 19:01 (Local time)). The wavelength range was 380 nm to 780 nm in 5 nm steps.

Here we describe how we use this database together with the blackbody radiators to study the influence of the statistical properties of the database on the resulting basis and consequently on the projection on the disk. In this experiment we computed the correlation matrix C_b from 50 blackbody radiation vectors in the range from 5000 K to 8000 K with equal spacing in the mired scale. Then we computed the correlation matrix C_N from the 21871 daylight spectra
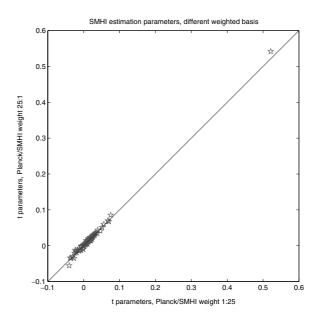
Weight for black body radiator: 1/Weight for daylight spectra: 25

Figure 6. Location of daylight spectra and Planck locus for correlation matrix $C_1 = 25C_N + C_b$ and SU(1,1) estimation.

Weight for black body radiator: 1/Weight for daylight spectra: 0.04

Figure 7. Location of daylight spectra and Planck locus for correlation matrix $C_2 = C_N + 25C_b$ and SU(1,1) estimation.

in the Norrköping database. In both cases the wavelength range was 380 nm to 780 nm in 5 nm steps. Next we combined these two matrices C_b, C_N and computed two new correlation matrices C_1, C_2. In the first case, Fig. 6, the relation between the daylight correlation matrix and the blackbody correlation matrix is (25:1), ie. $C_1 = 25C_N + C_b$ in the second case, Fig. 7, it was (1:25), ie. $C_2 = C_N + 25C_b$. Then we

projected the blackbody spectra and the spectra from one days observations (Norrköping, Sweden, March 10th, 1993, 8:45-11:15, 11:30-15:25, (local time), 5 minutes between two measurements, solar elevations between 8.6° and 23.3° and between 24.3° and 21.9° respectively) to the unit disk. In the blackbody dominated coordinate system the blackbody locus is nearer to the origin whereas the daylight sequence is nearer to the origin when the daylight spectra had weight factor 25 in the PCA. This is expected from the properties of the PCA but it has to be taken into account when interpreting the results obtained by this technique. Figures 6 and 7 show also the estimated **SU(1,1)** curves for each of the sequences. These two figures show that it was possible to estimate both sequences in both coordinate systems. The estimations are done using the Lie method for Planck locus in both cases and using the optimization method for the SMHI spectra. For each coordinate system we get an estimation of the curve parameters of the analyzed spectra. Comparing the results from both estimations we found that the time evolution parameters t for the SMHI spectra are in both cases closely related to each other (Fig. 8) by a multiplicative scale factor. This result is very natural since the coordinates of the points on the **SU(1,1)** curve are given by the parameters t and ξ_1, ξ_2, ξ_3 (see Eqs. (10) and (12)). Scaling the parameter t with a constant γ and the parameters ξ_1, ξ_2, ξ_3 with the inverse $1/\gamma$ leads to

Figure 8. Comparison of estimated t parameters computed from SMHI spectra in different coordinate systems.

the same coordinates and the description of the curve is thus only unique up to a scaling factor. We see that the estimations produce consistent results even though the estimations are done in different coordinate systems.

6. Discussion and Conclusions

The observation that illumination spectra can be described by a few coefficients in a suitable subspace is by now well-known. It is also known that these coefficients are all located in a cone-like subspace of the coefficient space. Empirically it has been demonstrated for a number of spectral databases that the space spanned by the first principal components together with the natural scaling of the axes provide such a conical parameterizations of the spectra in the database. The conical structure of the coefficient space can be exploited such that the value of the first coefficient is used as a norm of the spectrum, whereas the remaining coefficients provide an intensity-independent vector by perspective projection. This non-linear projection operation distinguishes the conical model from conventional subspace-based color descriptions. In the case of three-dimensional linear approximations this non-linear projection leads to coordinate vectors that are located on the unit disk and Lorentz-type transformations as their natural mappings.

Lorentz transformations have been used earlier to study color perception (see for example [1, 23, 33]) and some of those results are relevant in the current context. There are however also fundamental differences to the approach described here and in the following we point out some of them:

1. Earlier applications of group theoretical methods to color perception are based on the argument that changing conditions, such as illumination changes, map the color space into itself and that the boundary of the color space is invariant under these transformations. Some of these results are also valid here but the difference is that these models are intended to describe human color perception whereas the current methodology is completely data-driven and based on the properties of the spectral databases used.
2. Readers familiar with relativity theory may be tempted to identify the "spectral" cone with the cone in space-time. This is not correct since relativity theory deals with a four-dimensional space whereas spectral spaces are potentially infinite-dimensional. We deal with spectra, coordinates in conical sub-

sets of finite-dimensional vector spaces and the representatives of these coordinate vectors in the original Hilbert space and these three different objects have to be considered separately. A description of the relations between Lorentz groups and the group $SU(1,1)$ can be found in [31] (for example in Vol.1, Section 6.1.3).

In this paper we studied the properties of sets of blackbody spectra and databases of measured daylight spectra. We found for the blackbody radiators a close relation between the one-parameter subgroup description and the mired parametrization of the spectra. For the measured daylight spectra we showed that long stretches of the illumination spectra are located near one-parameter curves.

Although we did not derive an analytical relation between the spectral sequences and the one-parameter curves we found that the one-parameter curves provided good approximations of larger sets of illumination spectra. This observation should be useful in many image processing, computer vision and visualization applications. Here we mention a few examples:

1. *Visualization:* The color properties of an image point depend in general on the reflection properties of the object in the scene, the illumination and the sensor properties. If the dynamical spectral illumination characteristics can be modeled by a compact description like the one-parameter curves then this can be used in efficient color rendering of dynamical scenes.
2. *Estimation:* In many computer vision applications it is essential that the processing is independent of the illumination characteristics and depends only on the object properties. If the illumination changes can be described by one-parameter curves then this additional structure can be used for dynamical illumination compensation (dynamical color constancy).
3. *Compression:* Spectral illumination descriptions contain by definition all the physical information to characterize the illumination. They are however highly redundant. For this reason low-dimensional, parameterized descriptions of spectra are very useful. With the one-parameter curve description of sequences of spectra it is possible to reduce the redundancy of the coefficient-based descriptions further by taking into account the relation between related spectra.

In conclusion we found that the theory of one-parameter subgroups of Lie-groups provide powerful tools for approximation of dynamical sequences of illumination spectra. Motivated by the highly successful application of Lie-techniques in other areas of science and technology we find that their applications in color related problems in machine vision are very promising.

Appendix: Geometry of Spectral Spaces

In this appendix we give a new derivation of the conical properties of spectral color spaces and we also discuss the relation to earlier approaches to use Lorentz groups in color science.

In the following we denote by $I = [\lambda_{\min}, \lambda_{\max}]$ the closed interval of wavelengths of interest. The Hilbert space of square integrable functions on this interval is $H(I)$. The scalar product of elements f, g in the Hilbert space will be written as $\langle f, g \rangle$. We define a spectrum as an element in the Hilbert space with non-negative function values everywhere:

Definition 1.

1. $s(\lambda)$ is a spectrum if $s(\lambda) \geq 0$ for all $\lambda \in I$.
2. The space of all spectra is $\mathcal{C} = \{s(\lambda) \in H(I), s(\lambda)$ is a spectrum$\}$

For a finite set $\mathcal{B} = \{b_0(\lambda), \ldots, b_K(\lambda)\} \subset H(I)$ we define the projection operator $P_\mathcal{B} : H(I) \rightarrow \mathbb{R}^{K+1}, s \mapsto (\langle s, b_0 \rangle, \ldots \langle s, b_K \rangle) = (\sigma_0, \ldots \sigma_K) = P_\mathcal{B}(f)$. Starting from an element s in a Hilbert space and a given set $b_0, \ldots, b_K$ one can compute the coordinate vector $(\langle s, b_0 \rangle, \ldots, \langle s, b_K \rangle) = (\sigma_0, \ldots, \sigma_K)$. This mapping defines another mapping that maps an arbitrary coordinate vector $(\sigma_0, \ldots, \sigma_K)$ to the element $\tilde{s} = \sum_{k=0}^{K} \sigma_k b_k$ in the Hilbert space. For more information on how to apply the general theory of Hilbert spaces to signal processing the reader may consult [18].

In the Hilbert space we introduce a special type of projection operators which will lead to conical coordinate systems for spectra.

Definition 2. A conical basis consists of orthonormal functions $b_0, \ldots, b_K$ in $H(I)$ with the following properties:

1. There is a constant C_0 such that $b_0(\lambda) > C_0 > 0$ for all $\lambda \in I$.

2. There exists a constant C_1 such that for all $\lambda \in I$ and all unit vectors $u = (u_1, \ldots, u_K)$

$$\left| \sum_{k=1}^{K} u_k b_k(\lambda) \right| = b_u < C_1 \tag{30}$$

Since this definition is fundamental for the rest we make several remarks:

- It is enough to require the validity of the inequalities for all $\lambda \in I$ outside a set of measure zero. This allows basis functions with isolated singularities.
- The real restriction is the lower bound C_0 for the first basis function $b_0(\lambda)$.
- The restriction for the K basis functions $b_1, \ldots, b_K$ is not as severe since the closed interval I and the unit sphere in K dimensions are both compact.
- In our investigations we use only coordinate systems obtained by principal component analysis from data sets of spectra. For all investigated databases we found that the obtained bases were conical.

We now consider an arbitrary spectrum s and write it as

$$s = \langle s, b_0 \rangle b_0 + \langle s, b_1 \rangle b_1 + \cdots + \langle s, b_K \rangle b_K + s_e$$
$$= \sigma b_0 + \tau \left(\sum_{k=1}^{K} u_k b_k \right) + s_e \tag{31}$$

with unit vector $u = (u_1, \ldots, u_K)$. If the basis functions are conical it follows from the definition that there is a constant C such that

$$\left| \frac{\tau}{\sigma} \right| < C \tag{32}$$

To see this, note that from the definition follows: $\sigma = \langle s, b_o \rangle > C_0 \langle s, 1 \rangle$ where 1 is the function that has constant value one on the whole interval. Next define $u = (u_1, \ldots, u_K)$ as the unit vector in (31) and $b_u = \sum_{k=1}^{K} u_k b_k$. From the second property of the conical operator we find that $|\langle s, b_u \rangle| \leq C_1 \langle s, 1 \rangle$. Therefore we have

$$\left| \frac{\tau}{\sigma} \right| < \frac{C_1 \langle s, 1 \rangle}{C_0 \langle s, 1 \rangle} = \frac{C_1}{C_0} = C$$

Equation (32) shows:

Theorem 1. *If the basis is conical then the coordinate vectors of spectra are located in a cone.*

For a spectrum we now define the conical coordinate vector (σ, ρ, u) where $\rho = \tau/\sigma$ and σ, τ and u are defined as in Eq. (31).

Now assume we analyze spectra with a system characterized by a basis. When this system analyzes a spectrum s it represents it by the vector (σ, ρ, u). This mapping from the spectrum to coordinates is one of the main problems in traditional color science. In spectral based approaches it is however also important to consider the inverse mapping, ie. to define which functions should be represented by a given coordinate vector. Assume therefore that all such coordinate vectors should represent a spectrum. Among all the elements in the Hilbert space that are represented by this vector it is (in a Hilbert space framework) best to select the element $\tilde{s} = \sum_{k=0}^{K} \langle s, b_k \rangle b_k$. Since $\tilde{s}$ should represent a spectrum it seems plausible to define.

Definition 3. A coordinate vector $(\sigma, \rho, u) = (\sigma_0, \ldots, \sigma_K)$ is called admissible if the basis is conical and if $\sum_{k=0}^{K} \sigma_k b_k$ represents a spectrum, ie. is non-negative everywhere.

From the definition follows immediately that multiplication with a positive scalar maps an admissible vector to another admissible vector. We now show:

Theorem 2. *The space of admissible coordinate vectors is topologically equivalent to a product of the non-negative axis and the unit sphere.*

To see this we show that we can find a unique ρ_u such that all vectors $(1, \rho, u)$ with $\rho < \rho_u$ are admissible, while all vectors with $\rho > \rho_u$ are not. Consider a unit vector u and write:

$$s(\lambda) = s_{\sigma, \rho, u}(\lambda) = \sigma b_0(\lambda)\left(1 + \rho \frac{b_u(\lambda)}{b_0(\lambda)}\right)$$
$$\geq \sigma b_0(\lambda)(1 + \rho \beta_u) \tag{33}$$

where $\beta_u = \min_\lambda(b_u(\lambda)/b_0(\lambda))$. Since b_u and b_0 are orthogonal we see that $\beta_u < 0$. We also have $\sigma_0 = \langle s, b_0 \rangle \geq 0$ since s is non-negative and b_0 is positive everywhere. From this it follows that for all $b_u(\lambda)$ and for all $0 \leq \rho \leq -\beta_u^{-1}$ the function $s_{\sigma, \rho, u}(\lambda)$ is non-negative everywhere, i.e. it represents a spectrum. For $\rho > -\beta_u^{-1}$ the function $s_{\sigma, \rho, u}(\lambda)$ assumes negative values somewhere in the wavelength range. The boundary of the space of admissible coordinate vec-

tors in direction u is therefore given by $(\sigma, -\beta_u^{-1}, u)$. We call it the admissible boundary of the basis set.

Here we note that the relation between the boundary of the space of spectra and the boundary of the space of admissible coordinate vectors has to be analyzed carefully (for a detailed discussion of related topics see also [12]). The monochromatic spectra are certainly elements of the boundary in the spectral space, and the projection of the monochromatic spectra into coefficient space results in a curve called the spectral locus in traditional color science. Here it is important to point out that the spectral locus is not the boundary of the set of admissible coordinate vectors. This can be seen by considering the basis consisting of the three first trigonometric polynomials. The form of the spectral locus is also not limited to simple circle-like curves but can be much more difficult. We don't discuss this here but refer the reader to the examples discussed in [12].

Acknowledgments

References

1. M. Brill and G. West, "Group theory of chromatic adaptation," *Die Farbe*, Vol. 31, Nos. (1–3), pp. 4–22, 1983/84.

2. C.C. Chiao, T.W. Cronin, and D. Osorio, "Color signals in natural scenes: Characteristics of reflectance spectra and effects of natural illuminants," *J. Opt. Soc. Am. A*, Vol. 17, No. 2, pp. 218–224, 2000.

3. C.C. Chiao, D. Osorio, M. Vorobyev, and T.W. Cronin, "Characterization of natural illuminants in forests and the use of digital video data to reconstruct illuminant spectra," *J. Opt. Soc. Am. A*, Vol. 17, No. 10, pp. 1713–1721, 2000.

4. J. Cohen, "Dependency of the spectral reflectance curves of the Munsell color chips," *Psychon Science*, Vol. 1, pp. 369–370, 1964.

5. M. D'Zmura and Geoffrey Iverson, "Color constancy. I. Basic theory of two- stage linear recovery of spectral descriptions for lights and surfaces," *J. Opt. Soc. Am. A*, Vol. 10, pp. 2148–2165, 1993.

6. I.M. Gelfand, R.A. Minlos, and Z.Y. Shapiro, *Representations of the Rotation and Lorentz Groups and Their Applications*, Pergamon Press, 1963.

7. D. Gurarie, *Symmetries and Laplacians, Introduction to Harmonic Analysis, Group Representations and Applications*, vol. 174 of *North Holland Mathematics Studies*, North Holland, Amsterdam, London, New York and Tokyo, 1992.

8. S. Helgason, *Topics in Harmonic Analysis on Homogeneous Spaces*, vol. 13 of *Progress in Mathematics*, Birkhäuser: Boston-Basel-Stuttgart, 1981.

9. J. Hernández-Andrés, J. Romero, A. García-Beltrán, and J.L. Nieves, "Testing linear models on spectral daylight measurements," *Applied Optics*, Vol. 37, No. 6, pp. 971–977, 1998.

10. J. Hernández-Andrés, J. Romero, and R.L. Lee Jr, "Colorimetric and spectroradiometric characteristics of narrow-field-of-view clear skylight in Granada, Spain," *J. Opt. Soc. Am. A.*, Vol. 18, No. 2, pp. 412–420, 2001.

11. J. Hernández-Andrés, J. Romero, J.L. Nieves, and R.L. Lee Jr, "Color and spectral analysis of daylight in southern Europe," *J. Opt. Soc. Am. A.*, Vol. 18, No. 6, pp. 1325–1335, 2001.

12. J. Koenderinck and A. Kappers, "Color space," Technical Report (Report 16/96), Zentrum für interdiziplinäre Forschung der Universität Bielefeld, 1996.

13. R.L. Lee Jr, and J. Hernández-Andrés, "Measuring and modeling twilights purple light," *Applied Optics*, Vol. 42, No. 3, pp. 445–457, 2003.

14. R. Lenz, M. Österberg, J. Hiltunen, T. Jaaskelainen, and J. Parkkinen, "Unsupervised filtering of color spectra," *J. Opt. Soc. Am. A*, Vol. 13, No. 7, pp. 1315–1324, 1996.

15. R. Lenz, "Estimation of illumination characteristics," *IEEE Transactions Image Processing*, Vol. 10, No. 7, pp. 1031–1038, 2001.

16. R. Lenz, "Two stage principal component analysis of color," *IEEE Transactions Image Processing*, Vol. 11, No. 6, pp. 630–635, 2002.

17. R. Lenz, Linh Viet Tran, and Thanh Hai Bui, "Group theoretical invariants in color image processing," in *Proc. Eleventh Color Imaging Conference*, IS&T/SID, 2003, pp. 212–217.

18. S. Mallat, *A Wavelet Tour of Signal Processing*, Academic Press, 1999.

19. L.T. Maloney, "Evaluation of linear models of surface spectral reflectance with small numbers of parameters," *J. Opt. Soc. Am. A.*, Vol. 3, No. 10, pp. 1673–1683, 1986.

20. D.H. Marimont and B.A. Wandell, "Linear models of surface and illuminant spectra," *J. Opt. Soc. Am. A.*, Vol. 9, No. 11, pp. 1905–1913, 1992.

21. P.J. Olver, *Applications of Lie Groups to Differential Equations*, Springer: New York, 1986.

22. J.P.S. Parkkinen, J. Hallikainen, and T. Jaaskelainen, "Characteristic spectra of Munsell colors," *J. Opt. Soc. Am. A.*, Vol. 6, No. 2, pp. 318–322, 1989.

23. H.L. Resnikoff, "Differential geometry and color perception," *J. Mathematical Biology*, Vol. 1, pp. 97–131, 1974.

24. J. Romero, A. García-Beltrán, and J. Hernández-Andrés, "Linear bases for representation of natural and artificial illuminants," *J. Opt. Soc. Am. A*, Vol. 14, No. 5, pp. 1007–1014, 1997.

25. D.H. Sattinger and O.L. Weaver, *Lie Groups and Algebras with Applications to Physics, Geometry and Mechanics*, vol. 61 of *Applied Mathematical Sciences*, Springer, 1986.

26. C.L. Siegel, *Topics in Complex Function Theory*, vol. 2. Interscience tracts in pure and applied mathematics, 1969.

27. D. Slater and G. Healey, What is the spectral dimensionality of illumination functions in outdoor scenes? in *Proc. Conf. Computer Vision and Pattern Recognition*, IEEE Comp. Soc., 1998, pp. 105–110.

28. M. Sugiura, *Unitary Representations and Harmonic Analysis*, Kodansha Ltd., John Wiley and Sons, 1975.

29. S. Tominaga and B. A. Wandell, "Natural scene-illuminant estimation using the sensor correlation," in *Proceedings of the IEEE*, Vol. 90, No. 1, pp. 42–56, 2002.

30. S. Usui, S. Nakauchi, and M. Nakano, "Reconstruction of Munsell color space by a five-layer neural network," *J. Opt. Soc. Am. A*, Vol. 9, No. 4, pp. 516–520, 1992.

31. N.Ja. Vilenkin and A.U. Klimyk, *Representation of Lie Groups and Special Functions*, *Mathematics and its Applications*: 72. Kluwer Academic, 1991–1993.

32. G. Wyszecki and W.S. Stiles, *Color Science*, 2nd edition, Wiley & Sons: London, England, 1982.

33. H. Yilmaz, *On Color Perception*, vol. XX of *Int. School Physics, Enrico Fermi*, Academic Press, 1962, pp. 239–251.

Reiner Lenz is associate professor at the Department of Science and Technology, Linköping University, Sweden. He held positions as invited researcher at the ZEISS, Germany, the Advanced Telecommunication Research Institute (ATR), Kyoto, Japan, the Mechanical Engineering Laboratory, Tsukuba, Japan, Rutgers University, USA and AIST, Tsukuba, Japan. He received an honorable mention for the Pattern Recognition Society Award and the SAAB-Combitech Award. He is associated editor for Pattern Recognition and the IEEE-Transactions on Image Processing. He is interested in the application of group-theoretical methods in signal-, color-processing.

Thanh Hai Bui is currently a Ph.D. student at Media group, Institute of Science and Technology, Linköping University. He obtained his B.Sc. in Computer Science from Hanoi University of Technology in 1995, Post-graduate diploma in Manufacturing System Engineering from Asian Institute of Technology in 1999, Master of Applied Computer Science from Vrije Universiteit Brussel in 2000, and Ph. Licentiate in Media Technology from Linköping Universitet in 2003.

His work has mainly focused on multispectral database analysis, and applications of group theoretical methods.

Javier Hernández-Andrés received his Ph.D. degree in Physics from the University of Granada, Spain, in 1999. Since 2003 he is an associate professor in the Department of Optics at the same University. His research interests are color-image processing, multispectral color science, applied colorimetry, color vision and atmospheric optics.